

Optimization of lumping schemes for plane square quadratic finite element in elastodynamics

R. Kolman^{a,*}, J. Plešek^a, D. Gabriel^a, M. Okrouhlík^a

^a*Institute of Thermomechanics, AS CR, Dolejškova 5, 182 00 Praha 5, Czech Republic*

Received 7 September 2007; received in revised form 5 October 2007

Abstract

The effectiveness of explicit direct time-integration methods is conditioned by using diagonal mass matrix which entails significant computational savings and storage advantages. In recent years many procedures that produced diagonally lumped mass matrices were developed. For example, the row sum method and diagonal scaling method (HRZ procedure) can be mentioned. In this paper, the dispersive properties of different lumping matrices with variable mass distribution for the plane square 8-node serendipity elements are investigated. The dispersion diagrams for such lumping matrices are derived for various Courant numbers, wavelengths and the directions of wave propagation.

© 2007 University of West Bohemia. All rights reserved.

Keywords: wave propagation, dispersion analysis, serendipity finite elements, lumped mass matrix

1. Introduction

The numerical solution of the fast transient elastodynamics problem by the finite element method produces the dispersion errors: numerical attenuation or amplification, polarizations errors, numerical anisotropy, error in phase and group speeds, extraneous parasitic modes, numerical diffraction and scattering. These errors are induced by spatial and time discretizations. Accuracy of finite-element modelling is possible to influence by the choice of the element type, mesh size, time integration method, time step or modified mass matrix.

Krieg and Key [9] studied the one-dimensional constant strain elements for the numerical solution of the one-dimensional wave equation. Belytschko and Mullen [2] extended this dispersion analysis of one-dimensional elements to higher (quadratic) order for the Newmark's method and central difference method and consistent and lumped mass matrix. It was shown that a spurious branch in the spectrum existed. The existence of this branch caused the presence of noise associated with the propagation of discontinuities. In the textbook by Brillouin [3] on crystal periodic structures, the lowest branch was called the *acoustic* branch and the higher branches *optical* branches. A quite extensive paper was published by Abboud and Pinsky [1]. The authors analyzed the three-dimensional second-order scalar Helmholtz equation. The analysis was conducted for the trilinear rectangular 8-node elements, for the triquadratic rectangular

*Corresponding author. Tel.: +420 266 053 441, e-mail: kolman@it.cas.cz.

27-node elements and for the serendipity rectangular 20-node elements using various mass approximations.

In this paper, we follow up with recent author's work on the dispersion study [7, 10, 11, 8, 12], specifically the dispersion analysis of the numerical time-integration schemes [7]. The dispersive properties of different lumping matrices with variable mass distribution for the plane square 8-node serendipity elements are investigated. The optimal lumped mass matrix preserving the total element mass, physical symmetries and positivity is proposed.

2. Elastic plane waves

The i th equation of motion pertinent to linear elastodynamics reads

$$(\Lambda + G)u_{j,ji} + Gu_{i,jj} = \rho\ddot{u}_i \quad (1)$$

where Λ and G are Lamé's constants, ρ is density, u_i and \ddot{u}_i is i th component of the displacement vector and acceleration vector. Lamé's constants Λ and G can be expressed by engineering constants E, ν as

$$\Lambda = \frac{\nu E}{(1 + \nu)(1 - 2\nu)}, \quad G = \frac{E}{2(1 + \nu)}. \quad (2)$$

The analytical solution of the motion equation (1) for an unbounded isotropic continuum can be found in the closed form, two types of planar waves exist: the longitudinal wave and the transversal wave. The longitudinal wave propagates with the speed c_1 and the transversal wave propagates with the speed c_2 . The speeds c_1 and c_2 are given by relations

$$c_1 = \sqrt{\frac{\Lambda + 2G}{\rho}}, \quad c_2 = \sqrt{\frac{G}{\rho}}. \quad (3)$$

The time history of displacement of a plane harmonic solution reads

$$u_i = U_i(\mathbf{x}) \exp(ik(\mathbf{p} \cdot \mathbf{x} \pm ct)) = U_i(\mathbf{x}) \exp(i(\mathbf{k} \cdot \mathbf{x} \pm \omega t)), \quad i = 1, 2, \quad (4)$$

where t denotes time, k is the wave vector, \mathbf{p} is the unit normal to the wave front, $\mathbf{k} = k\mathbf{p}$ is the wave vector, c is the phase velocity, $\omega = c \cdot k$ is the angular velocity and U_i is i th component of the amplitude vector at the point defined by the position vector \mathbf{x} .

For a given wavelength λ , the wave number k may be computed from

$$k = \frac{2\pi}{\lambda}. \quad (5)$$

Finally, the group velocity c_g is defined as

$$c_g = \frac{d\omega}{dk}. \quad (6)$$

In non-dispersive systems, c is a constant and since $\omega = ck$, we get $c_g = c$. Thus, in the absence of dispersion the group velocity equals the phase velocity. On the other hand, $c_g \neq c$ indicates dispersion.

3. Finite element formulation

Spatial discretization by the finite element of an elastodynamics problem introduces the ordinary differential system

$$\mathbf{M}\ddot{\mathbf{q}} + \mathbf{K}\mathbf{q} = \mathbf{F}. \quad (7)$$

Here, \mathbf{M} is the mass matrix, \mathbf{K} the stiffness matrix, \mathbf{F} is the time-dependent load vector, the vectors \mathbf{q} and $\ddot{\mathbf{q}}$ contain nodal displacements and accelerations. The mass matrix \mathbf{M} and the stiffness matrix \mathbf{K} are defined by

$$\mathbf{M} = \int_V \rho \mathbf{N}^T \mathbf{N} dV, \quad \mathbf{K} = \int_V \mathbf{B}^T \mathbf{C} \mathbf{B} dV, \quad (8)$$

where ρ is the density, V is the volume, \mathbf{N} stores the displacement interpolation functions, \mathbf{B} denotes the strain-displacement matrix and \mathbf{C} is the elastic matrix. Under plane strain conditions, the elastic matrix \mathbf{C} takes on the form

$$\mathbf{C} = \frac{E}{1 - \nu^2} \begin{bmatrix} 1 & \nu & 0 \\ \nu & 1 & 0 \\ 0 & 0 & \frac{1-\nu^2}{2(1+\nu)} \end{bmatrix}. \quad (9)$$

In the subsequent analysis, a regular mesh $H \times H$ composed of plane square elements is considered. It proves useful to define reference matrices $\bar{\mathbf{M}}_e$, $\bar{\mathbf{K}}_e$ for a parent element having unit properties E and ρ , unit thickness b and unit length H . Then performing integration over the reference domain 1×1 one gets

$$\mathbf{K}_e = bE\bar{\mathbf{K}}_e, \quad \mathbf{M}_e = b\rho H^2\bar{\mathbf{M}}_e. \quad (10)$$

Therefore, a class of problems is defined by only the Poisson ratio ν . Within this class, the stiffness matrix $\bar{\mathbf{K}}_e$ is a function of ν whereas the mass matrix $\bar{\mathbf{M}}_e$ is independent of ν .

3.1. Central difference method

The central difference method is based on the approximation of the nodal velocities and nodal accelerations by relations

$$\dot{\mathbf{q}}^t = \frac{1}{2\Delta t} (\mathbf{q}^{t+\Delta t} - \mathbf{q}^{t-\Delta t}), \quad (11)$$

$$\ddot{\mathbf{q}}^t = \frac{1}{\Delta t^2} (\mathbf{q}^{t+\Delta t} - 2\mathbf{q}^t + \mathbf{q}^{t-\Delta t}), \quad (12)$$

where Δt denotes time step. The previous kinematic relations (11) and (12) prescribed in time t are substituted to the equation of motion (7) and the system of linear algebraic equations for solution of the nodal displacements $\mathbf{q}^{t+\Delta t}$ is obtained in the form

$$\mathbf{M}/\Delta t^2 \mathbf{q}^{t+\Delta t} = \mathbf{F}^t - (\mathbf{K} - 2\mathbf{M}/\Delta t^2) \mathbf{q}^t - (\mathbf{M}/\Delta t^2) \mathbf{q}^{t-\Delta t}. \quad (13)$$

Then, the nodal velocities $\dot{\mathbf{q}}^t$ and nodal accelerations $\ddot{\mathbf{q}}^t$ are computed from relations (11) and (12). Note that using the central difference method is especially effective for the diagonal mass matrix. In this case the inverse matrix \mathbf{M}^{-1} can be realized simply. More details about the stability and implementation of the central difference method can be found in [5].

3.2. Lumped mass algorithms

It is obvious that the diagonal mass matrix entails significant computational savings and storage advantages. In this section most used techniques that produce diagonally lumped mass matrices are summarized. The HRZ scheme [6] is an effective diagonal scaling method producing diagonal mass matrix in such way that the total element mass is preserved. Next approach uses the different shape functions for the derivation of the mass matrix (8), mostly the piecewise constant functions [4]. If the same shape functions are chosen identically with shape functions in the derivation of the stiffness matrix, the mass matrix is called the consistent mass matrix.

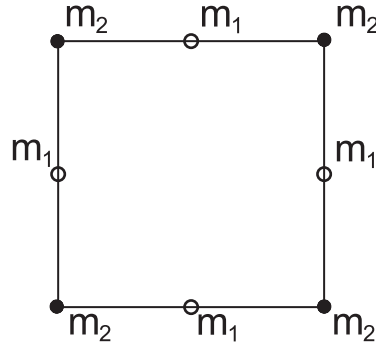


Fig. 1. General scheme of the mass distribution for 8-node serendipity square element.

Generally, the mass matrix must satisfy certain conditions: matrix symmetry, physical symmetries, conservation and positivity. Therefore, the diagonal components of the lumped mass matrix must be positive. Furthermore, the masses corresponding to the corner nodes and the masses corresponding to the midside nodes coincides for the square quadratic finite element (see Fig. 1). The condition for the keeping of the total element mass of the 8-node serendipity square finite element takes on the simple form

$$m = 4m_1 + 4m_2, \tag{14}$$

where m_1 denotes the mass of the midside node and m_2 is the mass of the corner node. If the mass corresponding to the midside node m_1 is chosen in the proportion to the total element mass m

$$m_1 = xm, \tag{15}$$

then for the mass of the corner node m_2 from the condition (14) holds

$$m_2 = (0.25 - x)m, \tag{16}$$

where x is the mass parameter. The value of the mass parameter x should be chosen in the range $(0, 0.25)$ requiring the positive definiteness of the mass matrix. The value $x = 8/36$ corresponds to the HRZ procedure with 2×2 Gauss quadrature, $x = 16/76$ the HRZ procedure with 3×3 Gauss quadrature and $x = 1/3$ to the row sum method. Note that the limit mass distribution occurs for $x = 0$ when full mass is inserted in the corner nodes and $x = 0.25$ when full mass is concentrated in the midside nodes. Next, the optimal value of mass parameter x will be determined based on the dispersion analysis.

4. Spatial time dispersion analysis

Since the finite element mesh is regular and uniform only the characteristic patch shown in Fig. 2 needs to be considered. Furthermore, one corner node $\{m, n\}$ and two mid-side nodes $\{m + 1, n\}$ and $\{m, n + 1\}$ must be taken into account when dealing with the serendipity mesh. In what follows, a characteristic segment of equations, which repeats itself in an unbounded mesh, is established. On it, a discrete pattern of harmonic waves is investigated.

Suppose, without loss of generality, that the origin of the coordinate system is located at node $\{m, n\}$. Thus, the nodal coordinates are given for the serendipity mesh

$$x_{m+p} = pH/2, \quad y_{n+q} = qH/2, \quad p, q = -2, -1, 0, 1, 2 \quad (17)$$

which is plotted in Fig. 2

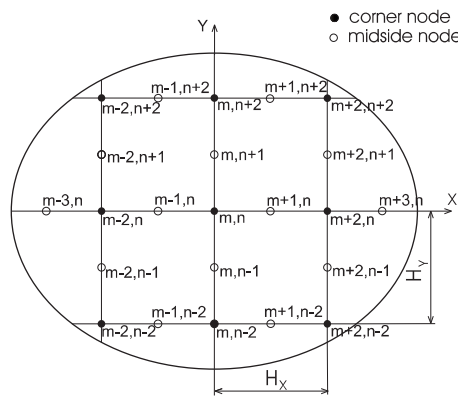


Fig. 2. Two dimensional serendipity regular finite element mesh.

The system of differential equation derived for the nodes of the considered patch can be written as

$$\mathbf{M}_c \ddot{\mathbf{q}}_c + \mathbf{K}_c \mathbf{q}_c = \mathbf{0} \quad (18)$$

where the local consistent mass matrix \mathbf{M}_c and the local stiffness matrix \mathbf{K}_c are of a rectangular form 6×42 for the serendipity finite element mesh. In the central difference method the discretized counterpart of (18) can be derived as

$$\left[\frac{1}{\Delta t^2} \mathbf{M}_c \right] \mathbf{q}_c^{t+\Delta t} + \left[\mathbf{K}_c + \frac{-2}{\Delta t^2} \mathbf{M}_c \right] \mathbf{q}_c^t + \left[\frac{1}{\Delta t^2} \mathbf{M}_c \right] \mathbf{q}_c^{t-\Delta t} = \mathbf{0} \quad (19)$$

with the aid of the relations (11), (12).

Next, the dispersion analysis follows when the prescribed nodal harmonic solution in the form

$$\begin{aligned} u_{mn} &= U_{mn} \exp [i (kx_m p_x + ky_n p_y - s \Delta t \omega)] \\ v_{mn} &= V_{mn} \exp [i (kx_m p_x + ky_n p_y - s \Delta t \omega)] \end{aligned} \quad (21)$$

is substituted to the differential equilibrium equations (18). In Eqn. (21) U_{mn} , V_{mn} define the shape of deformation mode and the discretized time t is defined as $t = s \Delta t$, where s is the multiple of the time step Δt . The components of vector \mathbf{p} are expressed by angle θ

$$p_x = \cos(\theta), \quad p_y = \cos(\pi/2 - \theta), \quad (22)$$

where angle θ is defined in Fig. 3.

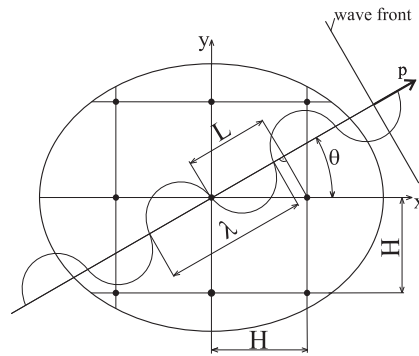


Fig. 3. Plane wave inclined by angle θ .

The time-harmonic nodal displacements (21) can be expressed in the symbolic form

$$u_{mn}^t = U_{mn} \cdot \mu_x^m \mu_y^n \mu_t^s, \quad v_{mn}^t = V_{mn} \cdot \mu_x^m \mu_y^n \mu_t^s, \quad (23)$$

$$\mu_x = \exp (i \alpha p_x), \quad \mu_y = \exp (i \alpha p_y), \quad \mu_t = \exp (i C \bar{\omega}), \quad \alpha = kH/2, \quad (24)$$

where Courant number $C = c_1 \Delta t / H$ and dimensionless angular velocity $\bar{\omega} = \omega H / c_1$ were used.

From above equations, the matrix form of the nodal displacements \mathbf{q}^t becomes simply by introducing the nodal amplitude vector \mathbf{U}_c

$$\mathbf{q}^t = \mathbf{D} \mathbf{A} \mathbf{U}_c \mu_x^m \mu_y^n \mu_t^s, \quad (25)$$

where the diagonal matrix \mathbf{D} stores from the product $\mu_x^i \mu_y^j$, the matrix \mathbf{A} mediates the affiliation of the characteristic nodal type. Finally, the dispersion relation is derived by (25), (10) and (19)

$$\left[(\mu_t - 2 + \mu_t^{-1}) \bar{\mathbf{M}}_c \mathbf{D} \mathbf{A} + C_0^2 \bar{\mathbf{K}}_c \mathbf{D} \mathbf{A} \right] \mathbf{U}_c = \mathbf{0}, \quad (26)$$

where $C_0 = c_0 \Delta t / H$ denotes the Courant number and $c_0 = \sqrt{E / \rho}$ is the speed in a bar.

For the given wavenumber k , the element size H and the angle of the propagation direction θ , the general eigenvalue problem is obtained in the form

$$\left(\hat{\lambda}\hat{\mathbf{M}} + \hat{\mathbf{K}}\right) \mathbf{U}_c = \mathbf{0}, \quad (27)$$

where

$$\hat{\mathbf{K}} = \bar{\mathbf{K}}_c \mathbf{D} \mathbf{A}, \quad \hat{\mathbf{M}} = \bar{\mathbf{M}}_c \mathbf{D} \mathbf{A}, \quad \hat{\lambda} = \frac{\mu_t - 2 + \mu_t^{-1}}{C_0^2}. \quad (28)$$

The dispersion relation $\bar{\omega} = f(kH, \theta, C)$ is then computed from

$$\bar{\omega} = \frac{1}{C} \text{Re}(-i \ln \hat{\mu}_t), \quad (29)$$

where $\hat{\mu}_t$ is given by

$$\hat{\mu}_{t1,2} = \frac{\hat{\lambda} C_0^2 + 2}{2} \pm \frac{\sqrt{(\hat{\lambda} C_0^2 + 2)^2 - 4}}{2} \quad (30)$$

using the value $\hat{\lambda}$ evaluated from (27). Note that only minus sign (30) is sufficient to take into account.

5. Results

The dispersion curves of the 8-node serendipity finite element for the consistent mass matrix and the exact time integration were presented in References [10],[11],[8]. Six dispersion curves $\bar{\omega} = f(kH, \theta, C)$ were obtained. The first and the second one are connected with the acoustic modes (longitudinal and transversal waves) while additional four ones are linked with the optical modes [3]. The type of waves is determined from the nodal amplitude values \mathbf{U}_c . For some frequency ranges the finite element mesh behaves like band-pass filters with discontinuity between individual frequency bands.

The numerical dispersion error can be measured by the ratio c/c_{exact} and c_g/c_{exact} or by the relative error $1 - c/c_{exact}$ and $1 - c_g/c_{exact}$. Since the dispersion error in the group speeds is more significant than in the phase speeds the criterion for the measurement of dispersion error is set to $1 - c_g/c_1$.

Comparison of dispersion properties of elements for various mass distribution given by the value of mass parameter x is shown in Fig. 4, where the relative error $1 - c_g/c_1$ versus the normalized wave length H/λ is drawn for different Courant numbers and the fixed angle $\theta = 0^\circ$. In Fig. 5 the dispersion behaviour of elements for various mass distribution is compared for different angle θ and the fixed Courant number $C = 0.5$. We observe that for the consistent mass matrix the dispersion error is smaller than 5% for the Courant number $C < 0.8$ and the wavelength $\lambda > 3H$ for arbitrary wave propagation. In case of diagonal mass matrix with the mass parameters $x \in (0.23, 0.25)$ the dispersion error is smaller than 10% for the Courant number $C < 0.8$ and the wavelength $\lambda > 5H$ for random wave propagation.

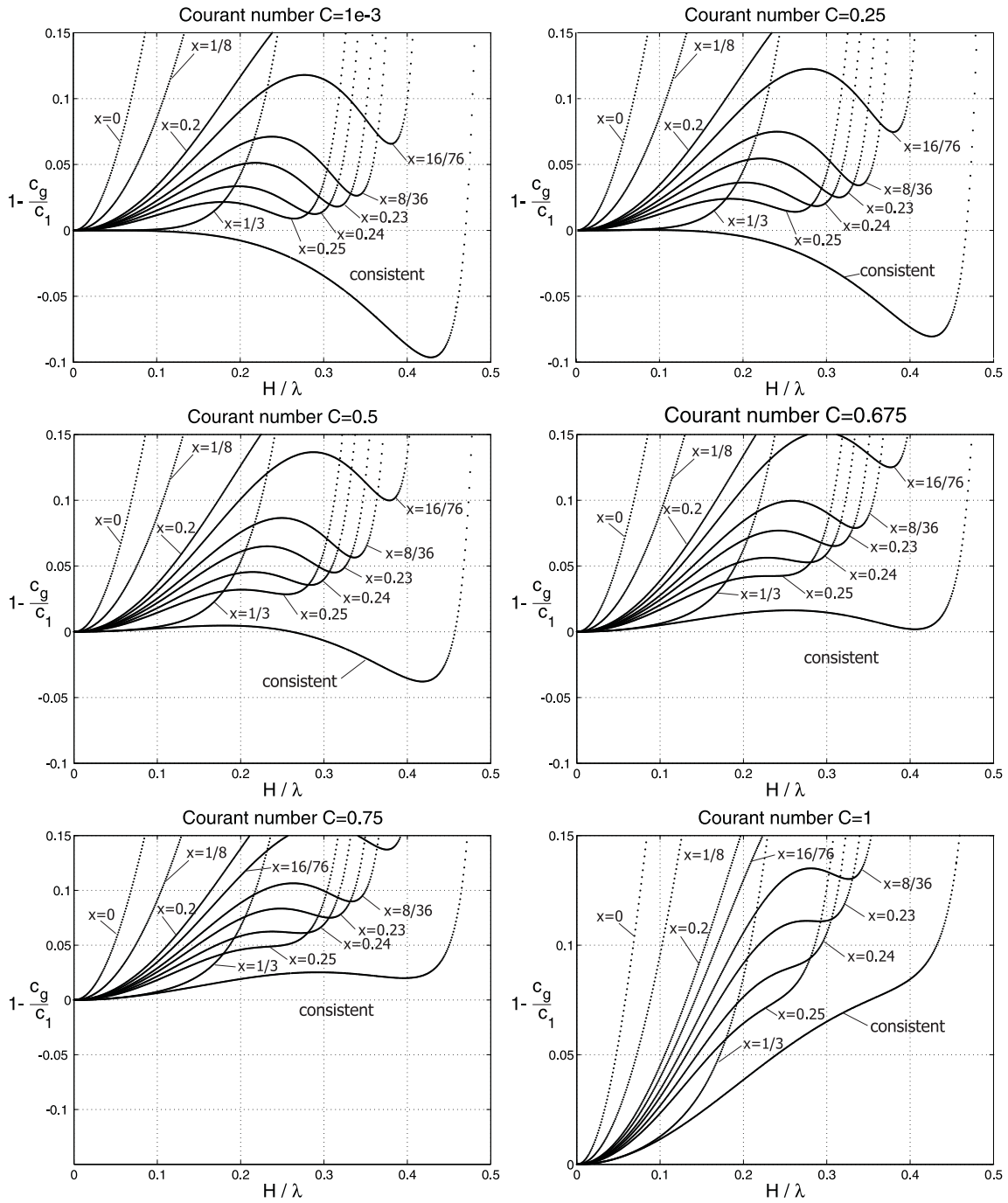


Fig. 4. Dispersion errors in the group speed of the longitudinal wave for $\theta = 0^\circ$, for the variable mass distribution and the variable Courant number. ($x=0$ – full mass is inserted in the corner nodes, $x = 1/4$ – full mass is in the midside nodes, $x = 1/8$ – the regular mass distribution, $x = 1/3$ – the row sum method, $x = 8/36$ – the HRZ procedure by 2 order Gauss quadrature, $x = 16/76$ by 3 order Gauss quadrature).

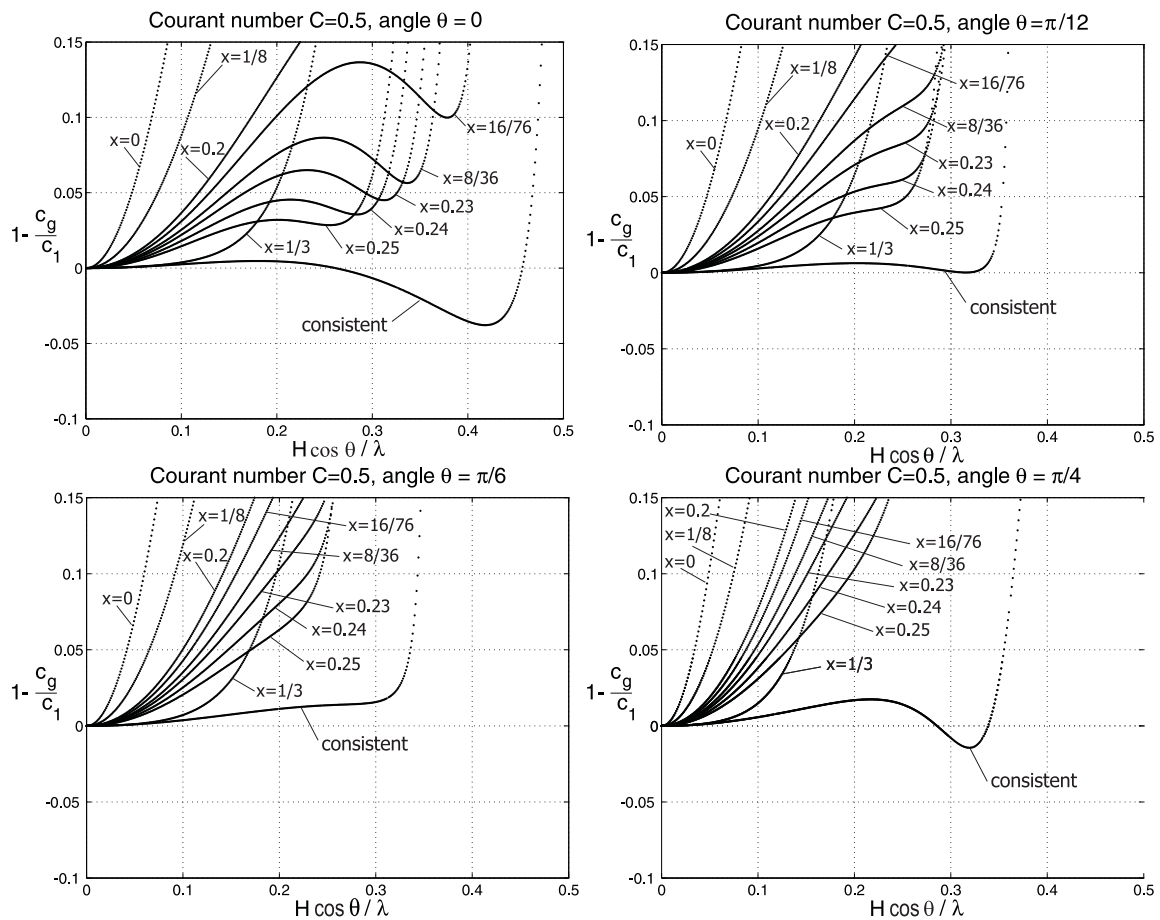


Fig. 5. Dispersion errors for the varied angle θ , the variable mass distribution and Courant number $C=0.5$. ($x=0$ – full mass is inserted in the corner nodes, $x = 1/4$ – full mass is in the midside nodes, $x = 1/8$ – the regular mass distribution, $x = 1/3$ – the row sum method, $x = 8/36$ – the HRZ procedure by 2 order Gauss quadrature, $x = 16/76$ by 3 order Gauss quadrature).

6. Conclusion

In this work the dispersive properties of different lumping matrices with variable mass distribution for the plane square 8-node serendipity elements were investigated. The dispersion diagrams for such lumping matrices were derived for various Courant numbers and the directions of wave propagation. It is concluded that the dispersion error is smaller than then 10% for the Courant number $C < 0.8$ and the wavelength $\lambda > 5H$ for elements whose mass distribution is more than 92% concentrated to the midside node independently on the wave propagation.

Acknowledgements

The work has been supported by the grant projects GA ĀR 101/07/1471 and 101/06/0914 in the framework of Acad. Sci. AV0Z20760514.

References

- [1] N.N. Abboud, P.M. Pinsky, Finite element dispersion analysis for the three-dimensional second-order scalar wave equation, *International Journal for Numerical Methods in Engineering* 35 (1992) 1183-1218.
- [2] T. Belytschko, R. Mullen, On dispersive properties of finite element solutions, *Modern problem in Elastic Wave Propagation*, 1978, pp. 67-82.
- [3] L. Brillouin, *Wave propagation in periodic structures: Electric filters and crystal lattices*, Dover Publications, New York, 1953.
- [4] R.W.Clough, Analysis of structural vibration and response, *Recent Advances in Matrix Methods of Structural Analysis and Desing*, Alabama Press, 1971, pp. 441-482.
- [5] M.A. Dokainish, K. Subbaraj, A survey of direct time-integration methods in computational structural dynamics - I. Explicit methods, *Computers and Structures* 32 (6) (1989) 1371-1386.
- [6] E. Hinton, T. Rock, O.C. Zienkiewicz, A note on mass lumping and related processes in the finite element method, *Earthquake Engineering and Structures Dynamics* 4 (1976) 245-249.
- [7] R. Kolman, M. Okrouhlík, J. Plešek, Effect of Time Integration on Dispersion Properties of Quadratic Finite Elements in Elastodynamics, *Computational Mechanics*, 2005, pp. 315-322.
- [8] R. Kolman, M. Okrouhlík, J. Plešek, Numerical tests of the dispersion properties of the quadratic finite elements in elastodynamics, *FEM Computation 2006*, Brno, 2006, pp. 7-16.
- [9] R.D. Krieg, S.W. Key, Transient shell response by numerical time integration, *International Journal for Numerical Methods in Engineering* 7 (1973) 273-286.
- [10] J. Plešek, R. Kolman, M. Okrouhlík, Numerical dispersion of quadratic finite element meshes, *WCCM VII, CDRUM, UCLA*, 2006.
- [11] J. Plešek, R. Kolman, M. Okrouhlík, On the occurrence of spurious opical modes in transient finite element analysis, *Mechanics & Materials in Design*, University of Porto, Porto, 2006, pp. 189-190.
- [12] J. Plešek, R. Kolman, D. Gabriel, F. Valeš, Application of dispersion analysis to the finite element solution of wave propagation and impact problems, *COMPDYN 2007, ECCOMAS 2007, Rethymno*, 2007.